

● *Original Contribution*

ROLE OF REACTIVE OXYGEN SPECIES DURING LOW-INTENSITY PULSED ULTRASOUND APPLICATION IN MC-3 T3 E1 PRE-OSTEOBLAST CELL CULTURE

HARMANPREET KAUR,* ARNO G. SIRAKI,[†] HASAN ULUDAĞ,[‡] DOUGLAS N. DEDERICH,[§] PATRICK FLOOD,[§] and TAREK EL-BIALY[¶]

*Department of Dentistry, University of Alberta, Edmonton, Alberta Canada; [†]Faculty of Pharmacy and Pharmaceutical Sciences, University of Alberta, Edmonton, Alberta, Canada; [‡]Department of Biomedical Engineering, Department of Chemical and Material Engineering, University of Alberta, Edmonton, Alberta, Canada; [§]Department of Dentistry, Faculty of Medicine and Dentistry, University of Alberta, Edmonton, Alberta, Canada; and [¶]Department of Dentistry, Department of Biomedical Engineering, University of Alberta, Edmonton, Alberta, Canada

(Received 16 December 2016; revised 2 June 2017; in final form 7 July 2017)

Abstract—We evaluated the activation of mitogen-activated protein kinase (MAPK) activation through reactive oxygen species (ROS) by application of low-intensity ultrasound (LIPUS) to MC-3 T3 E1 pre-osteoblasts. The cells were subjected to one LIPUS application for either 10 or 20 min, and the control group was exposed to a sham transducer. For ROS inhibition, 10 μ M diphenylene iodonium (DPI) was added to the cells an hour before LIPUS application. Samples were collected 1, 3, 6, 12 and 24 h after LIPUS application, and cells were evaluated for ROS generation, cell viability, gene expression and MAPK activation by immunoblot analyses. LIPUS caused a significant increase in ROS and cell viability in the non-DPI-treated group. Expression of *RUNX2*, *OCN* and *OPN* mRNA was higher in the LIPUS-treated groups at 1 h in both the DPI-treated and non-DPI-treated groups; *RUNX2* and *OCN* mRNA levels increased at 6 h. ERK1/2 activation was increased in the LIPUS-treated groups. These results indicate that LIPUS activates MAPK by ROS generation in MC-3 T3 E1 pre-osteoblasts. (E-mail: kaur3@ualberta.ca) © 2017 World Federation for Ultrasound in Medicine & Biology.

Key Words: Therapeutic ultrasound, Bone, Osteoblast, Reactive oxygen species, Mitogen-activated protein kinase.

INTRODUCTION

Osteoblasts are the fundamental bone-forming cells involved in bone matrix production and mineralization. These cells are equipped with special receptors that sense the change in the mechanical properties of the extracellular matrix and convert these signals to intra-cellular signaling through a mechanotransduction pathway. Integrins, G-protein receptors, stretch ion channels and mitogen-activated protein kinases (MAPKs) are the specific cellular components involved in mechanotransduction (Wang and Thampatty 2006). MAPKs constitute a primitive multifunctional signaling pathway that is involved in the regulation of bone mass and differentiation of osteoblasts. It consists of three serine–threonine kinases—extracellular signal-regulated kinase (ERK1/2), p38 and c-Jun N-terminal kinase (JNK)—that mediate

the response to a variety of stimuli. ERK1/2 is preferentially activated in response to growth factors, whereas p38 and JNK are more responsive to stress stimuli. Studies in mice with ERK1/2 germline deletion indicated that reduced bone mineralization (Matsushita et al. 2009) and p38 deletion lead to osteopenia in long bones (Beardmore et al. 2005). ERK1/2 and p38 have been found to exert their osteoblast differentiation effect by regulating phosphorylation of runt-related transcription factor 2 (RUNX2), which is a critical transcription factor for osteoblast differentiation, as well as gene and protein expression from osteoblast and hypertrophic chondrocytes (Greenblatt et al. 2010).

Hydrostatic pressure and cyclic compression are shear stresses that, as reported in the literature, can be used to apply mechanical stress in cell culture systems. One such method is the application of low-intensity pulsed ultrasound (LIPUS). Ultrasound has been used effectively in the medical field for more than five decades as a diagnostic, operative and therapeutic tool. *In vitro* studies have revealed increases in cell proliferation,

Address correspondence to: Harmanpreet Kaur, Department of Dentistry, Katz Group Centre for Pharmacy and Health Research, University of Alberta, 7-020, Edmonton, Alberta, Canada T6 G 2 E1. E-mail: kaur3@ualberta.ca

differentiation of osteoblasts, gingival fibroblasts, periodontal ligament cells and chondrocytes in response to LIPUS application (Tanaka et al. 2015). Because of the proliferative and angiogenic properties of LIPUS, recent studies have focused on its use for the treatment of osteoarthritis and bone regeneration as a supplementary method to scaffolds. Studies indicate that LIPUS application leads to integrin activation (Yang et al. 2005), calcium channel signaling (Parvizi et al. 2002) and intra-cellular activation of MAPKs and phosphatidylinositol 3-kinase (PI3K) (Tang et al. 2007). However, the potential mechanism of action of LIPUS on different cells is not fully understood.

Reactive oxygen species (ROS) are generated during aerobic cell metabolism through reduction–oxidation reactions. Since their discovery, ROS have been considered to have deleterious effects in living systems because of their involvement in aging, cancer metastasis and diabetic neuropathy (Krause 2007). It is only during the last decade that their favorable effects have been investigated in the cellular function as the second messenger in intracellular signaling engaged in proliferation and differentiation (Sauer et al. 2001). Indeed, they are considered harmful when generated at higher levels and cause oxidation of macromolecules like DNA, proteins and lipids through oxidative stress. Living tissues have a variety of enzymes and antioxidants, such as catalase, superoxide dismutase and glutathione, that keep a check on the levels of ROS generated. The level of ROS generated is a critical factor in cellular homeostasis. When generated at lower levels, ROS act as signaling molecules in cell growth and differentiation.

Nicotinamide adenine dinucleotide phosphate (NADPH) oxidases (NOX) are involved in ROS generation; there are seven subtypes, NOX1–NOX5 and the dual oxidases (DUOX1 and DUOX2), of which NOX2 and NOX4 are involved in bone homeostasis (Schröder 2014). These transmembrane proteins have in common conserved structural properties that like the carboxyl (–COOH)-terminal site, NADPH and flavin adenine dinucleotide (FAD) binding sites, six transmembrane domains, four heme-binding histidines and amine (–NH₂)-terminal transmembrane domains (Bedard and Krause 2007). ROS modify proteins composed of cysteine, methionine and selenocysteine. One such enzyme that is involved in MAPK functioning is protein tyrosine phosphatase (PTP), which is the target of ROS activity; hence, ROS are indirectly involved in MAPK activation (Son et al. 2013).

On the basis of this information, our aim was to investigate the effect of ROS generation during application of LIPUS to activate MAPK. We hypothesized that LIPUS stimulation increases ROS generation in MC-3 T3 E1 pre-osteoblasts, which in turn leads to MAPK

activation and increases gene expression of osteoblast-specific markers (*RUNX2*, *OCN* and *OPN*).

METHODS

Reagents

The MC-3 T3 E1 pre-osteoblast cell line was purchased from American Type Culture Collection (Manassas, VA, USA). Dulbecco's modified Eagle's medium/F12 (DMEM/F12) with L-glutamine and 4-(2-hydroxyethyl)-1-piperazineethanesulfonic acid (Hepes), fetal bovine serum (FBS), Dulbecco's phosphate-buffered saline (DPBS) and Hank's balanced salt solution (HBSS) were purchased from Life Technologies (Grand Island, NY, USA). Penicillin and streptomycin were purchased from Hyclone GE (Logan, UT, USA). Dihydroethidine (DHE), diphenylene iodonium (DPI), MTT [(3-(4, 5-dimethylthiazol-2-yl)-2, 5-diphenyltetrazolium bromide)], chloroform, isopropanol, bovine serum albumin (BSA) and dimethyl sulfoxide (DMSO) were purchased from Sigma Aldrich (St Louis, MO, USA). Sodium dodecyl sulfate, polyacrylamide and nitrocellulose membrane were purchased from Bio-Rad (Tokyo, Japan). A High-Capacity Reverse Transcription kit for cDNA preparation was purchased from Applied Biosystems (Foster City, CA, USA). Antibodies that were used in immunoblot analysis—anti-ERK1/2, anti-phospho-ERK1/2, anti-p38, anti-phospho-p38, anti-JNK, anti-phospho-JNK and horseradish peroxidase-conjugated anti-IgG—were purchased from Cell Signaling Technology (Danvers, MA, USA). For protein estimation, a Pierce BCA protein assay kit was purchased from Thermo Fisher (Rockford, IL, USA). An enhanced chemiluminescence (ECL) Western blot reagent kit was purchased from Amersham GE Health Care (Buckinghamshire, UK).

Cell culture

MC 3 T3 E1 mouse pre-osteoblast cells (1.5×10^5 /mL) were cultured in six-well plates (Thermo Fisher) in a medium containing DMEM/F12, 10% FBS, 50 units/mL penicillin and 50 μ g/mL streptomycin. Cells were incubated at 37°C in a humid chamber with 5% CO₂ and cultured for 24 h until the first LIPUS application. The cells were washed twice with DPBS and harvested 1, 3, 6, 12 and 24 h after LIPUS application to determine gene and protein expression. For ROS inhibition, DPI (10 μ M) was added to the cells cultured under similar cell density and conditions. DPI is a flavoprotein inhibitor that is best identified for NOX inhibition (Lambert et al. 2008) by extracting an electron from FAD or flavin mononucleotide to form a phenol radical, which reacts back with flavin to form a covalent phenylated adduct (Li et al. 2003b; Riganti et al. 2004). Before the addition of

DPI, cells were starved by removing the medium containing FBS and replacing it with DMEM/F12 only. DPI was added to DMEM/F12 at least 1 h before LIPUS application.

LIPUS application

Cells were exposed to LIPUS for either 10 or 20 min LIPUS; the control group was exposed to a sham transducer for similar periods. The LIPUS device was provided by Smile Sonica (Edmonton, AB, Canada) and was custom made for this experiment. The device generated 200- μ s bursts of 1.5-MHz sine waves with a pulse repetition frequency of 1 kHz and spatially averaged intensity of 30 mW/cm² of the transducer's surface area. These parameters have been used in our laboratory in the past (El-Bialy *et al.* 2006; Kaur *et al.* 2014, 2017). The six-well plates were placed on the surface of the transducer and coupling gel was applied to them for the transmission of ultrasound waves. Cells were divided into the following groups depending on LIPUS application and DPI addition: control DPI(–) with no LIPUS or DPI; LIPUS 10 min DPI(–) with 10 min of LIPUS and no DPI; LIPUS 20 min DPI(–) with 20 min of LIPUS and no DPI; control DPI(+) with no LIPUS, but with DPI; LIPUS 10 min DPI(+) with 10 min of LIPUS along with DPI; and LIPUS 20 min DPI(+) with 20 min of LIPUS in the presence of DPI.

Measurement of ROS production

The cells were washed with pre-warmed (37°C) DPBS solution and suspended in either DMEM/F12 (without phenol red) at a concentration of 1×10^5 /mL. The suspended cells were incubated with 25 μ M DHE for 20 min in the incubator before LIPUS application. Cells were sonicated with LIPUS according to the treatment groups, and 100 μ L of cell suspension was collected from each sample in triplicate at 0, 15, 30, 45, 60, 90 and 120 min and loaded in 96-blackwell plates (Thermo Fisher).

ROS have a very short half-life and hence it is difficult to measure them on long-term basis. Therefore, we measured ROS production at short intervals up to 2 h. Fluorescence intensity was quantified using a microplate reader (Tecan Infinite M200, Durham, NC, USA) with excitation and emission wavelengths of 480 and 570 nm, respectively. To study the effect of ROS inhibitor, 10 μ M DPI was added to the cell suspension, and the procedure was repeated.

Measurement of cell viability

Cells were seeded in a six-well plate (Thermo Fisher) in the presence and absence of DPI, and readings were taken 24 h after LIPUS application. The MTT assay was used as a measure of cell viability. Eight hundred

microliters of MTT solution (dissolved in HBSS using concentration of 5 mg/mL) was added to each well containing 2 mL of the medium and incubated for 2 h at 37°C. The medium was replaced with 2 mL of DMSO to dissolve MTT formazan crystals. Optical density was measured at 570 nm using a microplate reader (Tecan Infinite M200).

RNA extraction, cDNA synthesis and real-time qPCR

Total RNA was prepared using TRIzol reagent according to the manufacturer's instructions. RNA concentration was measured using the NanoDrop 2000 C spectrophotometer (Thermo Fisher, Wilmington, DE, USA). The first strand of cDNA was synthesized from 1 μ g total RNA by using the High-Capacity cDNA Reverse Transcriptase kit according to the instructions in a reaction volume of 20 μ L. After reverse transcription reaction, 1 of 10 dilutions was made from the template to be used in real-time qPCR. Ten microliters of real-time reaction mixture consisting of 3 μ L of cDNA, 1 μ L each of forward and reverse primers and 5 μ L of the master mix containing SYBR green dye was heated at 95°C for 2 min before undergoing 40 cycles of a denaturation step (15 s at 95°C) and an annealing step (1 min at 60°C) using the 7500 Real-Time PCR system (Applied Biosystems), during which the data were collected. Glyceraldehyde-3-phosphate dehydrogenase (GAPDH) was used as an internal control in each run. Normalized fluorescence was plotted against cycle number (amplification plot), and the threshold suggested by the software was used to calculate C_t (cycle at threshold). $\Delta\Delta C_t$ analysis was used to determine differences in gene expression compared with the control. The samples were collected from the groups 1, 3, 6, 12 and 24 h after LIPUS application. The primers used in the study are listed in Table 1.

Enzyme-linked immunosorbent assay for osteopontin detection

To determine the amount of OPN released, the supernatants were collected 1, 3, 6, 12 and 24 h after LIPUS exposure in the presence or absence of DPI. OPN enzyme-linked immunosorbent assay (ELISA) was performed according to the manufacturer's instructions. OPN concentration (pg/mL) was calculated from a standard curve.

Immunoblotting

For immunoblotting analysis, the pre-osteoblasts were cultured for 1, 3, 6, 12 and 24 h after a single ultrasound exposure. The cells were then washed with cold PBS twice and were lysed in Nonidet P-40 lysis buffer (50 mM Tris, pH 8.0, 150 mM NaCl, 1% Nonidet P-40 and freshly added 10^{-6} M protease inhibitor). The lysates were used as samples after centrifugation. Total protein

Table 1. Primers for real-time quantitative polymerase chain reaction

	Primer	Direction	Sequence (5' to 3')
1	RUNX2	Forward	GGGAACCAAGAAGGCACAGA
		Reverse	GGATGAGGAATGCGCCCTAA
2	OCN	Forward	GGCCAGACCTAGCAGACA
		Reverse	GGGCTTGGCATCTGTGAGG
3	OPN	Forward	GCAGCTCAGAGGAGAAGAAGC
		Reverse	TTCTGTGGCGCAAGGAGATT
4	NOX 2	Forward	TCATTCTGGTGTGGTTGGGG
		Reverse	CAGTGCTGACCCAAGGAGTT
5	NOX 4	Forward	ACCTCTGCCTGCTCATTGG
		Reverse	TCGCCCAACATTTGGTGAATG
6	GAPDH	Forward	GGAGAGTGTTCCTCGTCCC
		Reverse	CAAATGGCAGCCCTGGTGA

concentration was determined using the Pierce BCA kit. Cell lysates were separated on 12% polyacrylamide gels and blotted onto a nitrocellulose membrane. The membrane was blocked for 1 h at room temperature with 5% BSA in 1% TBS–Tween. After blocking, blots were probed with following primary antibodies (1:1000): phospho-ERK1/2, ERK1/2, phospho-p38, p38, phospho-JNK, JNK, β -actin in 5% BSA in 1% TBS–Tween overnight at 4°C. After incubation with HRP-conjugated anti-rabbit IgG (1:3000) for 1 h at room temperature, blots were washed and developed with ECL reagent. Blots were further visualized using the ChemiDoc MP Gel imaging system (Universal Hood III, Bio-Rad, Hercules, CA, USA), and the intensity of bands was quantitatively determined with ImageJ Software (National Institutes of Health, Bethesda, MD, USA). All tests were performed in triplicate.

Statistical analysis

The data are expressed as means \pm standard deviations, where the error bars represent standard deviations. Two statistical tests were applied: (i) A two-way repeated-measures analysis of variance (ANOVA) was followed by a *post hoc* Bonferroni test using SPSS Version 21.0 (IBM, Armonk, NY, USA) to determine significance for LIPUS applications and detection time. (ii) To study the effect of DPI at each time point, a one-way ANOVA followed by a Bonferroni *post hoc* test was used. The level of significance was set at $p < 0.05$.

RESULTS

ROS generation in MC-3 T3 E1 pre-osteoblast after LIPUS application

To investigate the effect of LIPUS application on ROS generation, we suspended the MC-3 T3 E1 cells in DMEM/F12 (phenol red free) at 1×10^5 cells/mL, incubated the cell suspension in 25 μ M DHE for 20 min and then applied LIPUS according to the assigned groups.

Samples were collected for fluorescence intensity measurement 0, 15, 30, 45, 60, 90 and 120 min after LIPUS (Fig. 1). DHE is superoxide-specific fluorescent dye that emits red fluorescence because of the formation of hydroxyethidine when oxidized by superoxide. LIPUS caused a significant increase in superoxide generation at all time points except 0 min (*i.e.*, immediately after LIPUS application) compared with the control group. LIPUS 10 min resulted in higher superoxide generation than LIPUS 20 min. For ROS inhibition, 10 μ M DPI was added to the cell suspension, which was then incubated with 25 μ M DHE for 20 min followed by LIPUS stimulation. DPI-treated groups exhibited a significant decrease in superoxide generation compared with non-DPI-treated groups. Unlike the non-DPI-treated group, the LIPUS 20 min group treated with DPI exhibited higher superoxide levels than the LIPUS 10 min and control groups.

Cell viability after LIPUS application

To study the effect of LIPUS application and ROS generation on cell viability, MC-3 T3 E1 cells were exposed to LIPUS in the presence or absence of DPI. After 24 h, cell viability was determined by MTT assay. In non-DPI-treated groups, there was a significant increase in MC-3 T3 E1 cell viability in the groups exposed to LIPUS compared with the control group. There was no difference in cell viability between the LIPUS 10 min and LIPUS 20 min groups. In DPI-treated groups, there was no statistical difference between the control and LIPUS groups. DPI treatment caused a significant decrease in viability of MC 3 T3 E1 pre-osteoblasts (Fig. 2).

Effect of LIPUS application on NOX2 and NOX4 mRNA expression

To investigate the effect of LIPUS stimulation on NOX2 and NOX 4 expression, MC-3 T3 E1 pre-osteoblasts were exposed to LIPUS, and samples were collected at 1, 3, 6, 12 and 24 h. For ROS inhibition, cells were first treated with 10 μ M DPI and then exposed to LIPUS. Expression of both NOX2 and NOX4 mRNA was significantly higher in DPI-treated groups at 1 h, after which expression level decreased. In the non-DPI-treated group, expression of NOX2 and NOX4 mRNA increased at 6 h. By 12 h, there was no significant difference in their expression levels (Figs. 3 and 4).

RUNX2, OCN and OPN mRNA expression after LIPUS application

To explore the effect of LIPUS stimulation and ROS inhibition, MC-3 T3 E1 cells were treated with LIPUS, and mRNA expression of osteoblast-specific markers was determined. In the non-DPI-treated group, RUNX2 expression was significantly increased in LIPUS groups

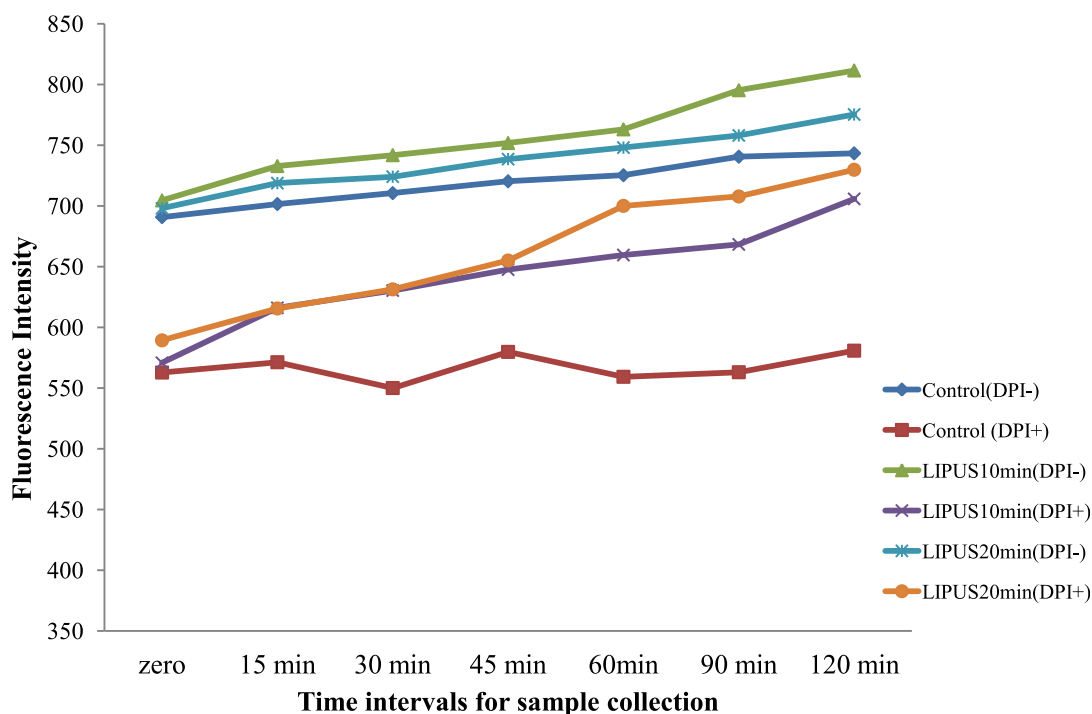


Fig. 1. Low-intensity pulsed ultrasound (LIPUS) stimulation induced generation of reactive oxygen species (ROS) in MC-3 T3 E1 pre-osteoblast cells. The cells were incubated with 25 μ M dihydroethidine (DHE) and sonicated with LIPUS according to the designated groups. For ROS inhibition, 10 μ M diphenylene iodonium (DPI) was added to Dulbecco's modified Eagle's medium/F12 (phenol red free). Samples were collected 0 (immediately after LIPUS application), 15, 30, 45, 60, 90 and 120 min after LIPUS application. The line graph depicts the time series of DHE fluorescence. LIPUS groups exhibited a significant increase in ROS generation from 15 min onward, whereas DPI-treated groups exhibited a significant decrease in ROS generation.

at 3, 6 and 12 h compared with the control group, whereas in the DPI-treated group, expression was highest during the first hour and then decreased at subsequent time points (Fig. 5).

In the non-DPI-treated group, LIPUS caused a significant increase in *OCN* mRNA expression at 1 and 24 h (Fig. 6a, b), whereas *OPN* caused a significant difference only at 1 h (Fig. 6c). In the DPI-treated group, expression of *OCN* and *OPN* mRNA was similar to that of *RUNX2*. LIPUS caused a significant increase in expression at 1 h compared with the control group. However, *OCN* expression decreased at 3, 6 and 12 h (Supplementary Fig. S1a-c, respectively) and *OPN* expression decreased at 3, 6, 12 and 24 h (Supplementary Fig. S2a-d, respectively; online only, available at <http://dx.doi.org/10.1016/j.ultrasmedbio.2017.07.002>).

Effect of LIPUS on OPN level

Changes in OPN protein levels after LIPUS application and ROS inhibition were determined using OPN ELISA by collecting the supernatants from the treatment groups at the previously mentioned time points. Contrary to gene expression, OPN protein level exhibited a

significant increase 1 h after LIPUS application in the non-DPI-treated group, whereas there was a significant decrease in the DPI-treated group. Nonetheless, protein levels were higher in non-DPI-treated groups after LIPUS application, but the differences were not statistically significant (Fig. 7).

MAPK activation after LIPUS application

To examine the effect of LIPUS application and ROS inhibition on MAPK activation, the cells were treated with LIPUS in the presence or absence of DPI. The cells were harvested at the previously mentioned time points. LIPUS stimulation resulted in a significant increase in ERK1/2 activation at 6, 12 and 24 h compared with the control in the non-DPI-treated group whereas DPI-treated cells exposed to LIPUS exhibited significant ERK1/2 activation at 1 h (Fig. 8). There were no significant differences in p38 and JNK activation levels in LIPUS-stimulated cells compared with control cells in both the DPI-treated and non-treated groups at any time points (Supplementary Figs. S3 and S4, online only, available at <http://dx.doi.org/10.1016/j.ultrasmedbio.2017.07.002>).

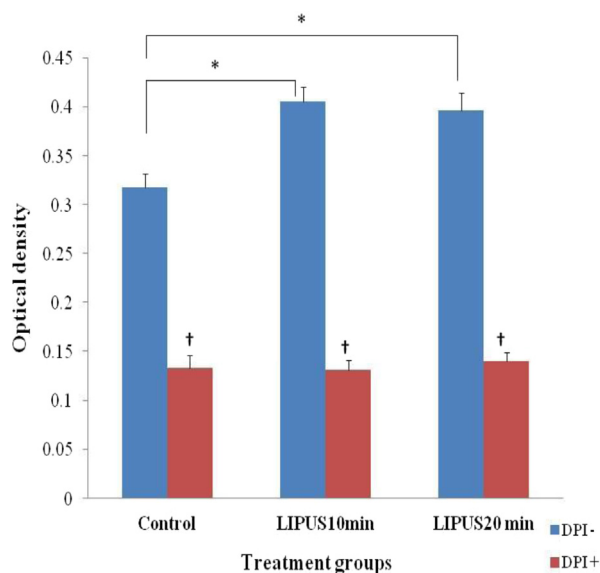


Fig. 2. Effect of low-intensity pulsed ultrasound (LIPUS) stimulation on viability of MC-3 T3 E1 pre-osteoblasts as measured by the MTT absorbance assay. After 24 h of LIPUS application in the presence and absence of 10 μ M diphenylene iodonium (DPI), the pre-osteoblasts were incubated in MTT solution (5 mg/mL dissolved in Hanks' balanced saline solution) for 2 h. The formazan crystals formed were dissolved in dimethyl sulfoxide, and absorbance was measured. Values in the bar graph are means \pm standard deviations. LIPUS stimulation caused a significant increase in cell viability compared with the control, whereas DPI-treated cells exhibited a significant decrease in viability. * $p < 0.05$, † $p < 0.05$ between the corresponding DPI-treated and non-treated cells.

DISCUSSION

Low-intensity pulsed ultrasound has been reported to increase cell proliferation and promote osteogenic differentiation of mesenchymal stem cells (Lv et al. 2013; Mostafa et al. 2009; Nagasaki et al. 2015). It has been routinely used in the medical field for the treatment of bone fractures (Busse et al. 2009; Hemery et al. 2011; Waseem et al. 2010). The mechanism underlying LIPUS is not completely understood. However, several attempts have been made to determine the mechanism underlying the interaction between LIPUS and the cell. On the basis of previous studies on the potential role of ROS in MAPK activation (Keshari et al. 2013; McCubrey et al. 2006; Son et al. 2013), we expected LIPUS stimulation to enhance the production of ROS that facilitate MAPK activation in MC-3 T3 E1 pre-osteoblasts. This would greatly expand our understanding of the use of LIPUS for fracture healing and, more recently, its use in tissue engineering and regenerative medicine.

We initially explored ROS generation in pre-osteoblasts using DHE. The effects of treatment with a

NOX inhibitor were also studied. DPI prevented the organization of NOX enzymes employed in ROS formation. Our study revealed a significant increase in ROS generation after LIPUS application, which was reduced when DPI was added to the cell culture. Similar results were obtained by Feril and Kondo (2005). However, our study is different as we used pulsed waves, while their study incorporated continuous waveforms. Also, in their study, the transducer was placed in the water bath to prevent an increase in temperature, whereas we used coupling gel to sonicate the cell. DHE is specific for superoxide ion, which is oxidized to form hydroxyl ion (OH^\cdot) and hydrogen peroxide (H_2O_2) in the presence of copper and ferrous ion through the Haber–Weiss reaction. H_2O_2 is a stable ROS product that can pass through the cell membrane and cause toxicity. Because ROS can harm cells through oxidative stress, MTT cell viability assay was employed to check for the toxicity of ROS generated after LIPUS application. Cell viability significantly increased in the LIPUS-exposed groups, indicating that the levels of ROS generated by LIPUS in the pre-osteoblast culture are not toxic under our experimental conditions.

Because our study noted an increase in ROS production and cell viability, our next step was to determine the expression of NOX enzymes involved in ROS production after LIPUS application. Hence, we stimulated MC-3 T3 E1 pre-osteoblasts with LIPUS and collected samples to determine expression of the *NOX2* and *NOX4* genes. We observed a significant increase in expression of both *NOX2* and *NOX4* at 6 h in the non-DPI-treated cells; interestingly, the expression of both genes was higher at 1 h in the DPI-treated cells. This may be attributed to the compensatory mechanism of the cells to generate higher gene levels in the case of inhibition.

NOX enzymes require the organization of additional components for activation: $\text{p}22^{\text{phox}}$, $\text{p}40^{\text{phox}}$, $\text{p}47^{\text{phox}}$ and $\text{p}60^{\text{phox}}$. The GTP-binding protein Rac1 is essential for NOX complex organization and activation (Bedard and Krause 2007). LIPUS has been reported to increase activation of Rac1 (Claire et al. 2009). In addition, BMP2, a potent bone-forming protein, has also been reported to increase ROS generation by activating NOX enzymes, and ROS inhibitors like *N*-acetylcysteine and DPI inhibited BMP2-induced ROS generation (Mandal et al. 2011). NOX2 and NOX4 play important roles in osteoblast proliferation and differentiation, respectively. Additionally, NOX4 protein expression was also higher in the osteoblast layer in subchondral bone of mandible condyle (Ambe et al. 2014). Collectively, these studies and our results indicate the involvement of both *NOX2* and *NOX4* for ROS production in cells during LIPUS application.

We subsequently investigated gene expression to explore the effects of ROS generated during LIPUS

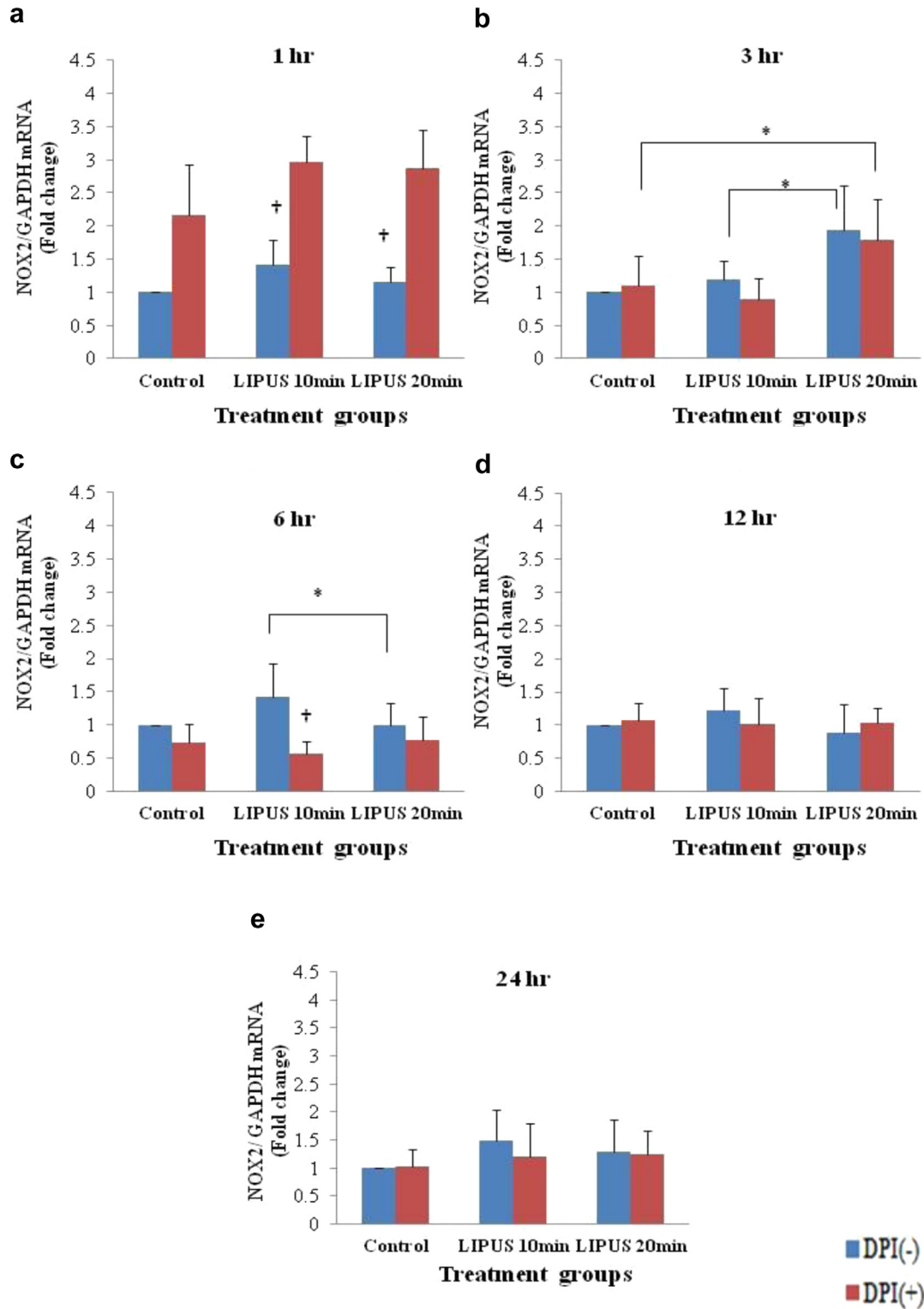


Fig. 3. Gene expression of NOX2 quantified by real-time quantitative polymerase chain reaction (RT-qPCR) in MC-3 T3 E1 pre-osteoblasts after application of low-intensity pulsed ultrasound (LIPUS) in the presence or absence of 10 μ M diphenylene iodonium (DPI). Samples were collected (a) 1 h, (b) 3 h, (c) 6 h, (d) 12 h and (e) 24 h after LIPUS application. The bar graph reveals a significant increase in NOX2 mRNA expression 1 and 3 h after LIPUS application in the DPI-treated cells, whereas there was a significant increase at 6 h in the non-DPI-treated cells. * $p < 0.05$, † $p < 0.05$ between the corresponding DPI-treated and non-treated cells.

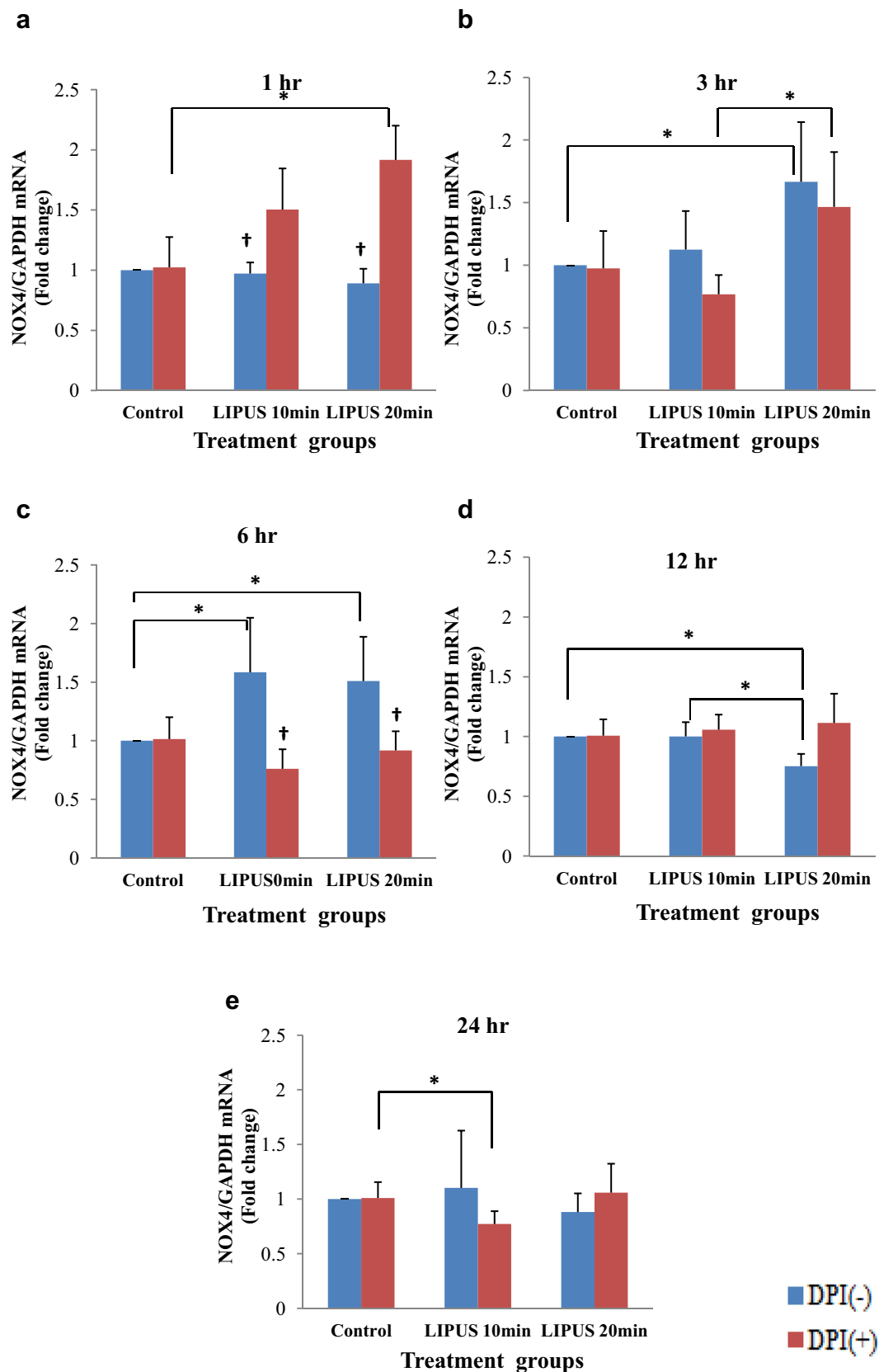


Fig. 4. Gene expression of *NOX4* quantified by real-time quantitative polymerase chain reaction (RT-qPCR) in MC-3 T3 E1 pre-osteoblasts after application of low-intensity pulsed ultrasound (LIPUS) in the presence or absence of 10 μ M diphenylene iodonium (DPI). Samples were collected (a) 1 h, (b) 3 h, (c) 6 h, (d) 12 h and (e) 24 h after LIPUS application. The bar graph reveals a significant increase in *NOX4* mRNA expression 1 and 3 h after LIPUS application in the DPI-treated cells, whereas there was significant increase at 6 h in the non-DPI-treated cells. * $p < 0.05$, † $p < 0.05$ between the corresponding DPI-treated and non-treated cells.

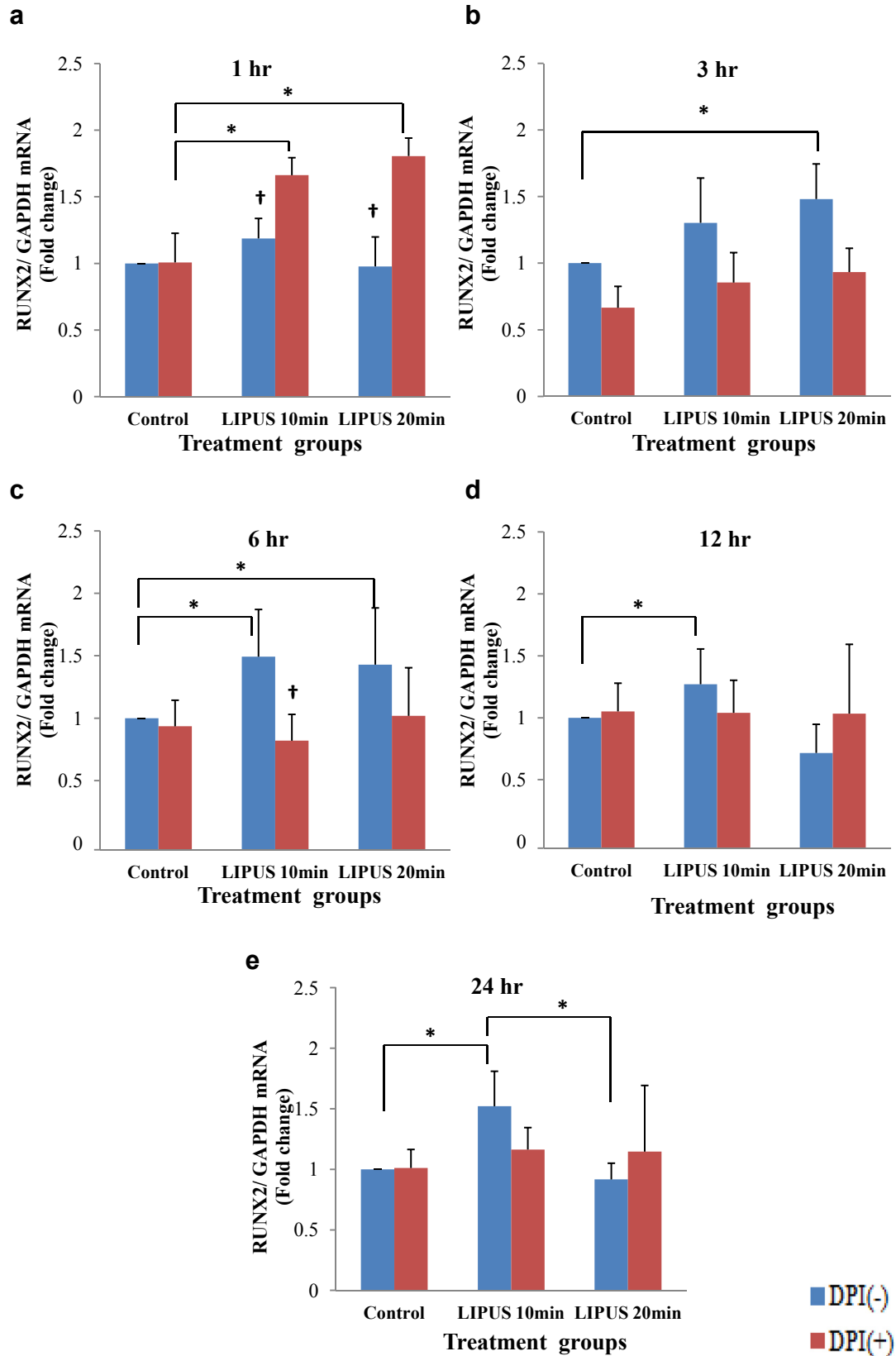


Fig. 5. *RUNX2* mRNA expression quantified using real-time quantitative polymerase chain reaction (RT-qPCR) in MC-3 T3 E1 pre-osteoblasts after application of low-intensity pulsed ultrasound (LIPUS) in the presence or absence of 10 μ M diphenylene iodonium (DPI). Samples were collected (a) 1 h, (b) 3 h, (c) 6 h, (d) 12 h and (e) 24 h after LIPUS application. The bar graph reveals a significant increase in *RUNX2* mRNA expression at 1 and 3 h in the LIPUS-treated cells compared with the control in the DPI-treated group, whereas the non-DPI-treated groups exhibited a significant increase in *RUNX2* expression at 6 and 12 h between control and LIPUS-treated cells. * $p < 0.05$, † $p < 0.05$ between the corresponding DPI-treated and non-treated cells.

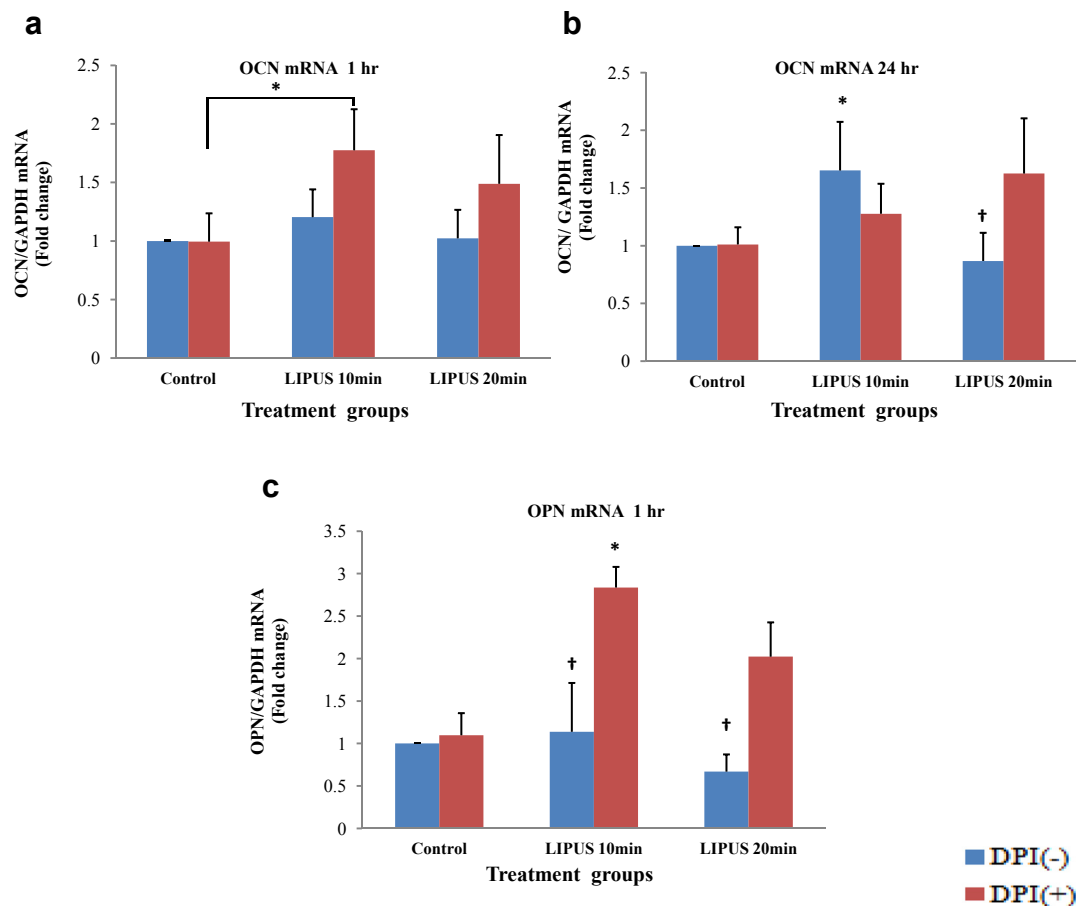


Fig. 6. Effect of low-intensity pulsed ultrasound (LIPUS) effect on expression of *OCN* and *OPN* mRNA. (a) The bar graph reveals a significant increase in *OCN* mRNA expression at 1 h in the LIPUS treated group compared with control in the diphenylene iodonium (DPI)-treated groups, (b) whereas the non-DPI-treated groups exhibited a significant increase in *OCN* expression at 24 h between the control and LIPUS-treated cells. (c) The bar graph reveals a significant increase in *OPN* mRNA expression in the LIPUS 10 min + DPI group compared with the other treatment groups. * $p < 0.05$, † $p < 0.05$ between the corresponding DPI-treated and non-treated groups.

application on pre-osteoblasts at the molecular level. *RUNX2* is a transcription factor that is essential for osteoblast differentiation and expression of osteoblast-specific genes and, consequently, is important for both intra-membranous and endochondral bone formation (Bruderer et al. 2014). *OCN* and *OPN* are late differentiation markers of osteoblasts. *OCN*, a non-collagenous protein, is secreted exclusively by osteoblasts that undergo carboxylation as a post-translational modification which helps it to bind to the mineralized bone matrix (Cooper et al. 2016). *OPN*, on the other hand, is a highly phosphorylated glycoprotein secreted by osteoblasts, hypertrophic chondrocytes and odontoblasts (Sodek et al. 2000). Our results indicated a significant increase in expression of *RUNX2* and *OCN* mRNA in LIPUS-treated cells compared with the control from 6 h onward for *RUNX2* and at 24 h for *OCN*. These results are supported by other studies on LIPUS-treated osteoblasts (Li et al. 2003a; Wu et al. 2015). In the ROS-inhibited

cells, expression of *RUNX2*, *OCN* and *OPN* mRNA was increased at 1 h. Furthermore, the protein level of *OPN* increased significantly after LIPUS exposure in non-DPI-treated cells, whereas the *OPN* level was significantly lower in DPI-treated cells during the first hour but changed significantly at later time points, reaching the same level as in the non-DPI-treated group by 24 h. Because *OPN* is a phosphorylated glycoprotein, gene expression was higher under ROS inhibition while the protein level was significantly lower. It is possible that ROS affected the phosphorylation of *OPN*. To the best of our knowledge, no study has reported the interaction between *OPN* and ROS in osteoblasts.

It has been suggested that mechanical stimuli play a crucial role in MAPK activation in different cell lines. In osteoblasts, ERK1/2 is involved in *OCN* and bone sialoprotein (BSP) expression through *RUNX2* activation. Also, ERK1/2 is involved in post-translational modification of cytoskeleton, which helps in cell migration.

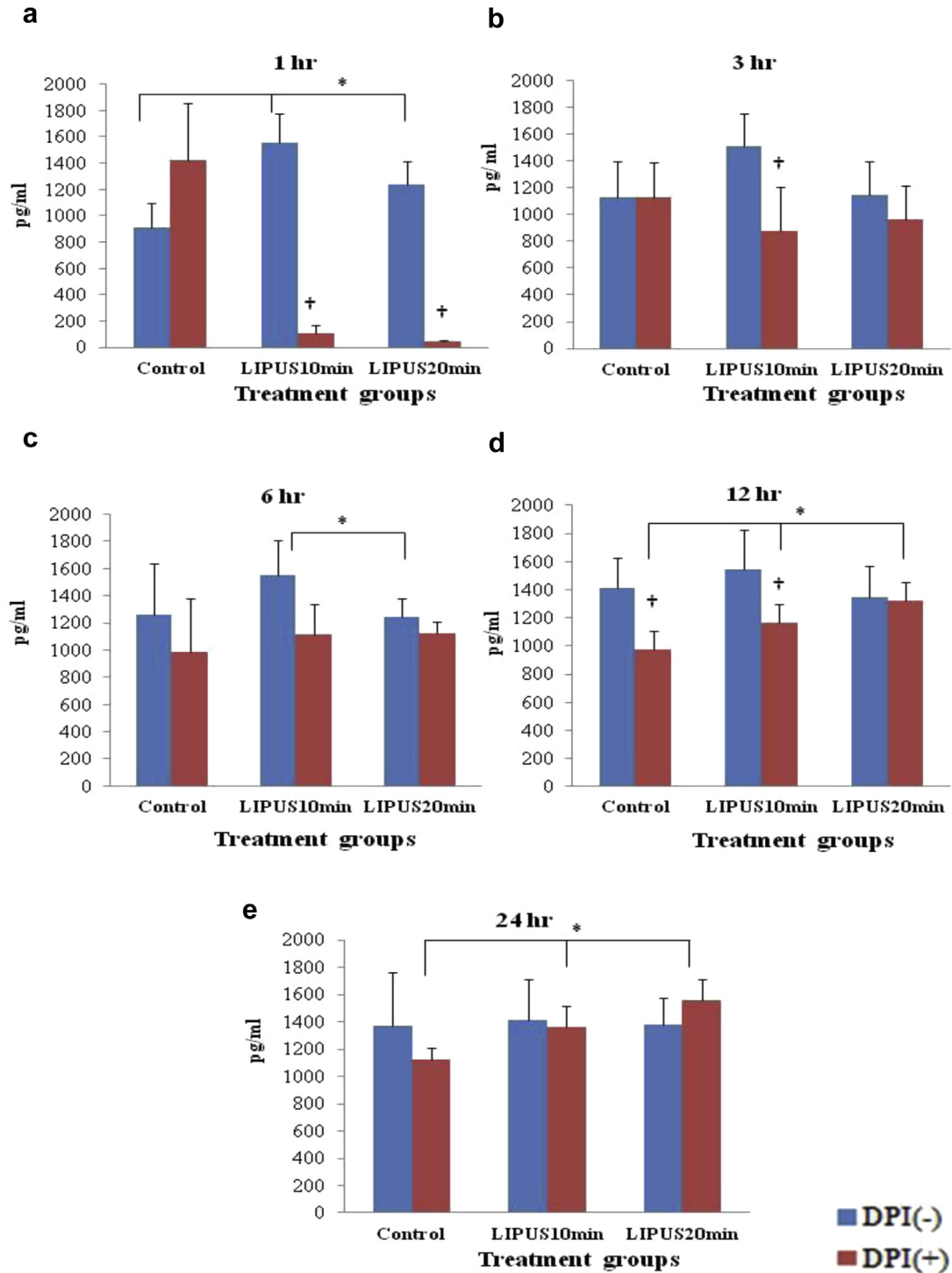


Fig. 7. Effect of exposure to low-intensity pulsed ultrasound (LIPUS) on OPN protein expression at (a) 1 h (b) 3 h (c) 6 h (d) 12 h and (e) 24 h was measured by enzyme-linked immunosorbent assay. The supernatants were collected after LIPUS exposure. In the non-DPI-treated group, LIPUS caused a significant increase in OPN protein expression, whereas in the DPI-treated group, the level of ROS significantly decreased during the first hour. With the passage of time, the levels of expression in DPI-treated and non-treated groups became equal. * $p < 0.05$, [†] $p < 0.05$ between the corresponding DPI-treated and non-treated groups.

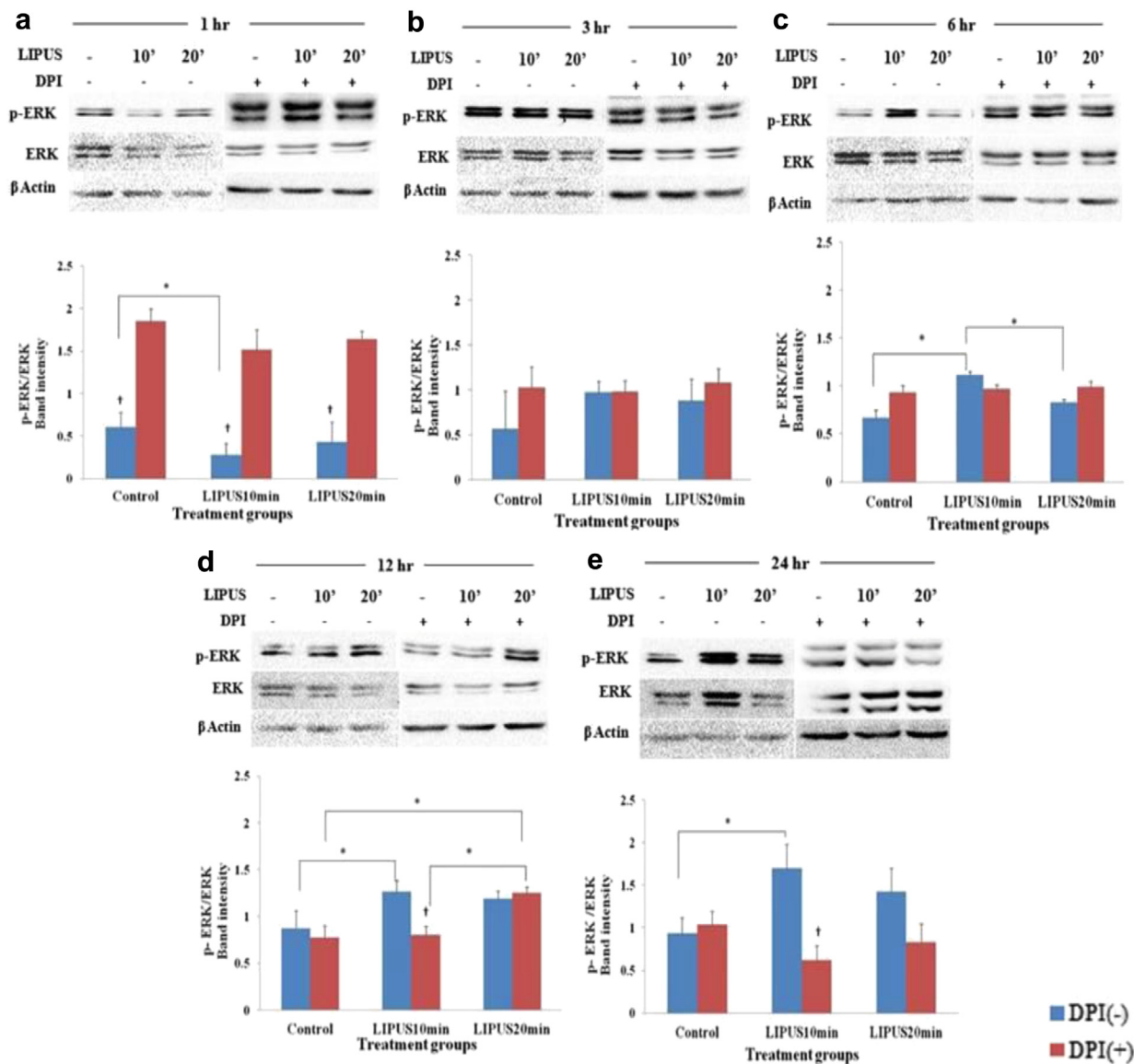


Fig. 8. ERK1/2 activation after low-intensity pulsed ultrasound (LIPUS) application assessed by immunoblot analysis. MC-3 T3 E1 pre-osteoblasts were treated with LIPUS in the presence or absence of 10 μ M diphenylene iodonium (DPI). Samples were harvested for immunoblot analysis (a) 1 h, (b) 3 h, (c) 6 h, (d) 12 h and (e) 24 h after LIPUS application. The level of phosphorylation of ERK1/2 relative to total ERK1/2 was determined by quantification of the band intensity using ImageJ software. LIPUS groups exhibited a significant increase in the phosphorylation level at 6 h, 12 h and 24 h in the non-DPI-treated group, whereas the phosphorylation level significantly increased at 1 h in the DPI-treated group and then decreased at later time points. * $p < 0.05$, † $p < 0.05$ between the corresponding DPI-treated and non-treated groups.

Similar to ERK, p38 promotes osteoblast differentiation; however, JNK activation in osteoblasts is not completely understood. An *in vitro* study of JNK inhibition reduced the expression of BSP and OCN and blocked late-stage osteoblast differentiation (Greenblatt et al. 2013). Finally, we determined if the MAPK signaling pathway is activated in MC-3 T3 E1 pre-osteoblasts after LIPUS exposure. Our study found increased ERK1/2 activation in LIPUS-exposed, non-DPI-treated cells from 6 h onward, whereas ROS inhibition led to early activation of ERK1/2.

Because ERK1/2 is involved in *RUNX2* activation, the results of *RUNX2* gene expression followed a trend similar to that for ERK1/2 activation. These results strongly suggest that ERK1/2 activation after LIPUS stimulation is involved in *RUNX2* expression.

Our aim in this study was to gain an understanding of the mechanism underlying LIPUS in MC-3 T3 E1 pre-osteoblasts. Therapeutic ultrasound has been used extensively for imaging fetuses and crushing calculi in the urinary tract and in surgical procedures like

lumpectomies. Its application is based on the intensity used, ranging from a low of 30 mW/cm² to a high of 300 W/cm². Therapeutic ultrasound exerts thermal and non-thermal effects on the bone. However, the intensity of 30 mW/cm² used in LIPUS is considered too low to generate a thermal effect. In the present study we used 30 mW/cm² intensity as it has been approved by the U.S. Food and Drug Administration for bone fracture healing (Bashardoust *et al.* 2012; Leung *et al.* 2004). It is recommended that future studies use higher intensities to collect more information on ROS generation and cell signaling at higher intensities.

The non-thermal effect is further divided into cavitation and acoustic streaming. Cavitation involves the generation of gas bubbles in tissue fluid, which oscillate with compression and rarefaction of ultrasound waves and collapse to generate a small amount of energy (Claes and Willie 2007), thus causing damage to the cell (Johns 2002). Like the thermal effect, the intensity of LIPUS is too low to generate cavitation in the bone. Another non-thermal effect by which LIPUS benefits the bone is the generation of a fluid flow along and around the cell membrane. These waves cause radiation forces on the membrane and affect mechanosensitive receptors like integrins (Padilla *et al.* 2014), as well as change the micro-environment around the cell by changing concentration gradients of ions, stretching ion channels and improving the distribution of growth factors (Ebisawa *et al.* 2004). Mechanical stimulation of LIPUS activates integrins (Yang *et al.* 2005) that further trigger phosphorylation of focal adhesion molecules like focal adhesion kinase and Src (de Gusmão *et al.* 2009; Zhou *et al.* 2008), which are upstream regulators of MAPK signaling. Recent studies have found that phosphorylation of MAPK and focal adhesion molecules is controlled by reversible redox modification. ROS oxidize the thiol group in the focal adhesion molecule and in PTPs, thus causing conformational changes by forming disulfide bonds (Fernandes *et al.* 2014).

In this study, we tested LIPUS for two durations, 10 and 20 min, to optimize the time for *in vitro* study. The 20-min LIPUS application is most frequently used in *in vivo* studies and is also approved by the U.S. Food and Drug Administration for fracture healing, whereas most *in vitro* studies have found an increased anabolic effect of LIPUS at 10 min. This could be due to attenuation of LIPUS during passage through living tissue. On the other hand, in *in vitro* studies, there is less attenuation. Also, we placed the cell culture plates on the transducer surface using coupling gel as a transfer medium. With this setup, a temperature increase $\leq 3^{\circ}\text{C}$ for a 20-min application has been reported by Leskinen and Hynynen (2012). This temperature increase might have also caused a difference in LIPUS effects at the molecular

level. Intra-membranous ossification and endochondral ossification are two processes of bone formation. Previously, it was believed that hypertrophic chondrocytes undergo apoptosis and die, but recent studies have reported differentiation of chondrocytes into osteoblasts (Jing *et al.* 2015). Gentili *et al.* (1993) found that chondrocytes, when cultured in the presence of ascorbic acid (another ROS scavenger), differentiated into osteoblast-like cells. In endochondral bone formation, ROS and ERK1/2 are involved in the differentiation of chondrocytes (Chen *et al.* 2015; Morita *et al.* 2007). At present, we can only hypothesize ROS to be another factor that can regulate chondrocyte differentiation.

CONCLUSIONS

Our study indicates that LIPUS regulates the expression of osteogenic-specific genes and activation of the ERK1/2 signaling pathway *via* ROS generation in MC-3 T3 E1 pre-osteoblast cells. Further studies are needed to understand the role of ROS in endochondral ossification.

Acknowledgments—This study was supported in part by the McIntyre Fund, Department of Dentistry, Faculty of Medicine and Dentistry, University of Alberta, and Dr. Hasan Uludag, Department of Biomedical Engineering, Department of Chemical and Material Engineering, University of Alberta.

SUPPLEMENTARY DATA

Supplementary data related to this article can be found online at <http://dx.doi.org/10.1016/j.ultrasmedbio.2017.07.002>.

REFERENCES

- Ambe K, Watanabe H, Takahashi S, Nakagawa T. Immunohistochemical localization of Nox1, Nox4 and Mn-SOD in mouse femur during endochondral ossification. *Tissue Cell* 2014;46:433–438.
- Bashardoust TS, Houghton P, MacDermid JC, Grewal R. Effects of low-intensity pulsed ultrasound therapy on fracture healing: A systematic review and meta-analysis. *Am J Phys Med Rehabil* 2012;91:349–367.
- Beardmore VA, Hinton HJ, Eftychi C, Apostolaki M, Armaka M, Darragh J, McIlrath J, Carr JM, Armit LJ, Clatcher C, Malone L, Kollias G, Arthur JSC. Generation and characterization of p38 β (MAPK11) gene-targeted mice. *Mol Cell Biol* 2005;25:10454–10464.
- Bedard K, Krause KH. The NOX family of ROS-generating NADPH oxidases: Physiology and pathophysiology. *Physiol Rev* 2007;87:245–313.
- Bruderer M, Richards RG, Alini M, Stoddart MJ. Role and regulation of RUNX2 in osteogenesis. *Eur Cell Mater* 2014;28:269–286.
- Busse JW, Kaur J, Mollon B, Bhandari M, Tornetta P III, Schünemann HJ, Guyatt GH. Low intensity pulsed ultrasonography for fractures: Systematic review of randomised controlled trials. *BMJ* 2009;338:b351.
- Chen Z, Yue SX, Zhou G, Greenfield EM, Murakami S. ERK1 and ERK2 regulate chondrocyte terminal differentiation during endochondral bone formation. *J Bone Miner Res* 2015;30:765–774.
- Claes L, Willie B. The enhancement of bone regeneration by ultrasound. *Prog Biophys Mol Biol* 2007;93:384–398.

- Claire MM, Morgan MR, Harrison A, Humphries MJ, Bass MD. Therapeutic ultrasound bypasses canonical syndecan-4 signaling to activate rac1. *J Biol Chem* 2009;284:8898–8909.
- Cooper MS, Seibel MJ, Zhou H. Glucocorticoids, bone and energy metabolism. *Bone* 2016;82:64–68.
- Ebisawa K, Hata K, Okada K, Kimata K, Ueda M, Torii S, Watanabe H. Ultrasound enhances transforming growth factor β -mediated chondrocyte differentiation of human mesenchymal stem cells. *Tissue Eng* 2004;10:921–929.
- El-Bialy T, Hassan A, Albaghdadi T, Fouad HA, Maimani AR. Growth modification of the mandible with ultrasound in baboons: A preliminary report. *Am J Orthod Dentofacial Orthop* 2006;130:435.e7–435.e14.
- Feril LB, Kondo T. Major factors involved in the inhibition of ultrasound-induced free radical production and cell killing by pre-sonication incubation or by high cell density. *Ultrason Sonochem* 2005;12:353–357.
- Fernandes GVO, Cavagis ADM, Ferreira CV, Olej B, Leão MDS, Yano CL, Peppelenbosch M, Granjeiro JM, Zambuzzi WF. Osteoblast adhesion dynamics: A possible role for ROS and LMW-PTP. *J Cell Biochem* 2014;115:1063–1069.
- Gentili C, Bianco P, Neri M, Malpeli M, Campanile G, Castagnola P, Cancedda R, Cancedda FD. Cell proliferation, extracellular matrix mineralization, and ovotransferrin transient expression during in vitro differentiation of chick hypertrophic chondrocytes into osteoblast-like cells. *J Cell Biol* 1993;122:703–712.
- Greenblatt MB, Shim JH, Zou W, Sitara D, Schweitzer M, Hu D, Lotinun S, Sano Y, Baron R, Park JM, Arthur S, Xie M, Schneider M, Zhai B, Ggyi S, Davis R, Glimcher LH. The p38 MAPK pathway is essential for skeletogenesis and bone homeostasis in mice. *J Clin Invest* 2010;120:2457–2473.
- Greenblatt MB, Shim JH, Glimcher LH. Mitogen-activated protein kinase pathways in osteoblasts. *Annu Rev Cell Dev Biol* 2013;29:63–79.
- de Gusmão CVB, Pauli JR, Saad MJA, Alves JM, Belangero WD. Low-intensity ultrasound increases FAK, ERK-1/2, and IRS-1 expression of intact rat bones in a noncumulative manner. *Clin Orthop Relat Res* 2009;468:1149–1156.
- Hemery X, Ohl X, Saddiki R, Barresi L, Dehoux E. Low-intensity pulsed ultrasound for non-union treatment: A 14-case series evaluation. *Orthop Traumatol Surg Res* 2011;97:51–57.
- Jing Y, Zhou X, Han X, Jing J, von der Mark K, Wang J, de Crombrughe B, Hinton RJ, Feng JQ. Chondrocytes directly transform into bone cells in mandibular condyle growth. *J Dent Res* 2015;94:1668–1675.
- Johns LD. Nonthermal effects of therapeutic ultrasound: The frequency resonance hypothesis. *J Athl Train* 2002;37:293–299.
- Kaur H, Uludağ H, El-Bialy T. Effect of nonviral plasmid delivered basic fibroblast growth factor and low intensity pulsed ultrasound on mandibular condylar growth: A preliminary study. *Biomed Res Int* 2014;4:26710.
- Kaur H, Uludağ H, Dederich DN, El-Bialy T. Effect of increasing low-intensity pulsed ultrasound and a functional appliance on the mandibular condyle in growing rats. *J Ultrasound Med* 2017;36:109–120.
- Keshari RS, Verma A, Barthwal MK, Dikshit M. Reactive oxygen species-induced activation of ERK and p38 MAPK mediates PMA-induced NETs release from human neutrophils. *J Cell Biochem* 2013;114:532–540.
- Krause KH. Aging: A revisited theory based on free radicals generated by NOX family NADPH oxidases. *Exp Gerontol* 2007;42:256–262.
- Lambert AJ, Buckingham JA, Boysen HM, Brand MD. Diphenyleneiodonium acutely inhibits reactive oxygen species production by mitochondrial complex I during reverse, but not forward electron transport. *Biochim Biophys Acta* 2008;1777:397–403.
- Leskinen JJ, Hynynen K. Study of factors affecting the magnitude and nature of ultrasound exposure with in vitro set-ups. *Ultrasound Med Biol* 2012;38:777–794.
- Leung KS, Lee WS, Tsui HF, Liu PPL, Cheung WH. Complex tibial fracture outcomes following treatment with low-intensity pulsed ultrasound. *Ultrasound Med Biol* 2004;30:389–395.
- Li JK, Chang WH, Lin JC, Ruaan RC, Liu HC, Sun JS. Cytokine release from osteoblasts in response to ultrasound stimulation. *Biomaterials* 2003a;24:2379–2385.
- Li N, Ragheb K, Lawler G, Sturgis J, Rajwa B, Melendez JA, Robinson JP. DPI induces mitochondrial superoxide-mediated apoptosis. *Free Radic Biol Med* 2003b;34:465–477.
- Lv Y, Zhao P, Chen G, Sha Y, Yang L. Effects of low-intensity pulsed ultrasound on cell viability, proliferation and neural differentiation of induced pluripotent stem cells-derived neural crest stem cells. *Biotechnol Lett* 2013;35:2201–2212.
- Mandal CC, Ganapathy S, Gorin Y, Mahadev K, Block K, Abboud HE, Harris SE, Choudhury GG, Choudhury NG. Reactive oxygen species derived from Nox4 mediate BMP2 gene transcription and osteoblast differentiation. *Biochem J* 2011;433:393–402.
- Matsushita T, Chan YY, Kawanami A, Balmes G, Landreth GE, Murakami S. Extracellular signal-regulated kinase 1 (ERK1) and ERK2 play essential roles in osteoblast differentiation and in supporting osteoclastogenesis. *Mol Cell Biol* 2009;29:5843–5857.
- McCubrey JA, LaHair MM, Franklin RA. Reactive oxygen species-induced activation of the MAP Kinase signaling pathways. *Antioxid Redox Signal* 2006;8:1775–1789.
- Morita K, Miyamoto T, Fujita N, Kubota Y, Ito K, Takubo K, Miyamoto K, Ninomiya K, Suzuki T, Iwasaki R, Yagi M, Takashi H, Toyama Y, Suda T. Reactive oxygen species induce chondrocyte hypertrophy in endochondral ossification. *J Exp Med* 2007;204:1613–1623.
- Mostafa NZ, Uludağ H, Dederich DN, Doschak MR, El-Bialy TH. Anabolic effects of low-intensity pulsed ultrasound on human gingival fibroblasts. *Arch Oral Biol* 2009;54:743–748.
- Nagasaki R, Mukudai Y, Yoshizawa Y, Nagasaki M, Shiogama S, Suzuki M, Kondo S, Shintani S, Shirota T. A combination of low-intensity pulsed ultrasound and nanohydroxyapatite concordantly enhances osteogenesis of adipose-derived stem cells from buccal fat pad. *Cell Med* 2015;7:123–131.
- Padilla F, Puts R, Vico L, Raum K. Stimulation of bone repair with ultrasound: A review of the possible mechanic effects. *Ultrasonics* 2014;54:1125–1145.
- Parvizi J, Parpura V, Greenleaf JF, Bolander ME. Calcium signaling is required for ultrasound-stimulated aggrecan synthesis by rat chondrocytes. *J Orthop Res* 2002;20:51–57.
- Riganti C, Gazzano E, Polimeni M, Costamagna C, Bosia A, Ghigo D. Diphenyleneiodonium inhibits the cell redox metabolism and induces oxidative stress. *J Biol Chem* 2004;279:47726–47731.
- Sauer H, Wartenberg M, Hescheler J. Reactive oxygen species as intracellular messengers during cell growth and differentiation. *Cell Physiol Biochem* 2001;11:173–186.
- Schröder K. NADPH oxidases in bone homeostasis and osteoporosis. *Cell Mol Life Sci* 2014;72:25–38.
- Sodek J, Ganss B, McKee MD. Osteopontin. *Crit Rev Oral Biol Med* 2000;11:279–303.
- Son Y, Kim S, Chung HT, Pae HO. Reactive oxygen species in the activation of MAP kinases. In: Cadenas E, Packer L, (eds). *Methods in enzymology*. New York: Academic Press; 2013. p. 27–48.
- Tanaka E, Kuroda S, Horiuchi S, Tabata A, El-Bialy T. Low-intensity pulsed ultrasound in dentofacial tissue engineering. *Ann Biomed Eng* 2015;43:871–886.
- Tang CH, Lu DY, Tan TW, Fu WM, Yang RS. Ultrasound induces hypoxia-inducible factor-1 activation and inducible nitric-oxide synthase expression through the integrin/integrin-linked kinase/Akt/mammalian target of rapamycin pathway in osteoblasts. *J Biol Chem* 2007;282:25406–25415.
- Wang JHC, Thampatty BP. An introductory review of cell mechanobiology. *Biomech Model Mechanobiol* 2006;5:1–16.
- Waseem Z, Ford M, Syed K, Flannery J. Chronic nonunion in a patient with bilateral supracondylar distal femur fractures treated successfully with twice daily low intensity pulsed ultrasound. *PM R* 2010;2:159–161.
- Wu L, Lin L, Qin YX. Enhancement of cell ingrowth, proliferation, and early differentiation in a three-dimensional silicon carbide scaffold using low-intensity pulsed ultrasound. *Tissue Eng Part A* 2015;21:53–61.
- Yang RS, Lin WL, Chen YZ, Tang CH, Huang TH, Lu BY, Fu WM. Regulation by ultrasound treatment on the integrin expression and differentiation of osteoblasts. *Bone* 2005;36:276–283.
- Zhou S, Bachem MG, Seufferlein T, Li Y, Gross HJ, Schmelz A. Low intensity pulsed ultrasound accelerates macrophage phagocytosis by a pathway that requires actin polymerization, Rho, and Src/MAPKs activity. *Cell Signal* 2008;20:695–704.